JOURNAL OF MATERIALS SCIENCE 27 (1992) 2291–2297

Modified triglycine sulphate (TGS) single crystals for pyroelectric infrared detector applications

M. BANAN‡, R. B. LAL, ASHOK BATRA
Department of Physics, Alabama A & M University, P.O. Box 71, Normal, AL 35762, USA

Effect of caesium and cerium, L-alanine and caesium + L-alanine impurities are investigated on ferroelectric and pyroelectric properties of TGS crystals. Dielectric constant and loss, pyroelectric coefficient, spontaneous polarization and coercive field measurements of these modified crystals, as a function of temperature are reported. Caesium and cerium did not affect the electrical properties of TGS crystals significantly, whereas L-alanine- and, especially, Cs + L-alanine-doped TGS crystals exhibited promising improvements in pyroelectric properties, up to 48 °C, as compared to pure TGS crystals.

1. Introduction

Triglycine sulphate (TGS) is an organic ferroelectric material having a second-order phase transition at the Curie point of about 49 °C with its polar axis along the monoclinic *b*-axis [1–3]. A survey of a number of possible materials for use in pyroelectric detectors shows that TGS and its derivatives are interesting and promising materials. TGS crystals have exhibited applications for pyroelectric thermal imaging and room-temperature infrared detection is a wide spectrum range of 8–14 μm [4, 5], as compared to quantum detectors which require cryogenic operating temperatures and possess a narrow spectrum range of operation [6]. These are the unique advantages for the cost-effective use of TGS detectors in military systems, astronomical telescopes, earth observation cameras, environmental analyses monitors and Fourier transform infrared (FTIR) instrumentation. The current interest in TGS crystals for thermal imaging and detecting devices has promoted the need for crystals of high optical quality with improved pyroelectric properties. The detectivity, D^*, presently obtained from a TGS pyroelectric chip is more than an order of magnitude lower than an ideal thermal radiation noise-limited performance. Many efforts have been made [7–11] and are being made to improve the pyroelectric properties and growth of TGS crystals [12–14] for use in commercial and laboratory applications. TGS crystals were also grown in low-gravity environment aboard the Spacelab-3 mission of the National Aeronautics and Space Administration of United States of America to investigate the growth kinetics and pyroelectric performance [15].

The objective of the present work was to investigate the effects of L-alanine (organic dipolar molecule), caesium and cerium ions (transition metal and rare earth ion, respectively), and simultaneously doping L-alanine + caesium ion on the ferroelectric and pyroelectric properties of TGS crystals. Using these properties/parameters, applicable figures of merits of modified TGS crystals for use in detectors and vidicons are calculated for comparison over pure TGS crystals.

2. Experimental procedure

Single crystals of pure and doped crystals were grown from aqueous solution by a temperature-lowering technique using a modified version of a reciprocating crystallizer [16], shown in Fig. 1. The saturated solution of TGS, at 40 °C, was prepared using BDH optran grade crystalline powder. The optimum amount of impurities were added by weight to the starting saturated solution. The impurities used were L-alanine, caesium sulphate, cerium sulphate, and L-alanine + cesium sulphate. The growth solution containing required impurities was equilibrated in the crystallizer at 42 °C for 48 h. The temperature of the crystallizer was maintained at ± 0.01 °C. The appropriate polyhedral seed crystals were affixed to the seed holder with a Dow Corning silicone adhesive. The seed crystals and the holder were preheated to 42 °C before insertion into the growth cell. The crystal surface was allowed to dissolve slightly then the temperature was lowered to the correct saturation temperature and held constant for 24 h. Afterwards, it was lowered at a programmed rate, which increased from the initial 0.1 °C day^{-1} to 0.30 °C day^{-1}. All the growth parameters, i.e. saturation temperation (about 40 °C), weight of the solution, impurity concentration, weight of the seed, rate of temperature lowering (degree of supersaturation) and the rate of seed rotation were kept identical during the growth of pure and doped crystals so as to balance out the effect of growth

‡*Present address*: Department of Chemical Engineering, Clarkson University, Potsdam, NY 13676, USA.

0022–2461

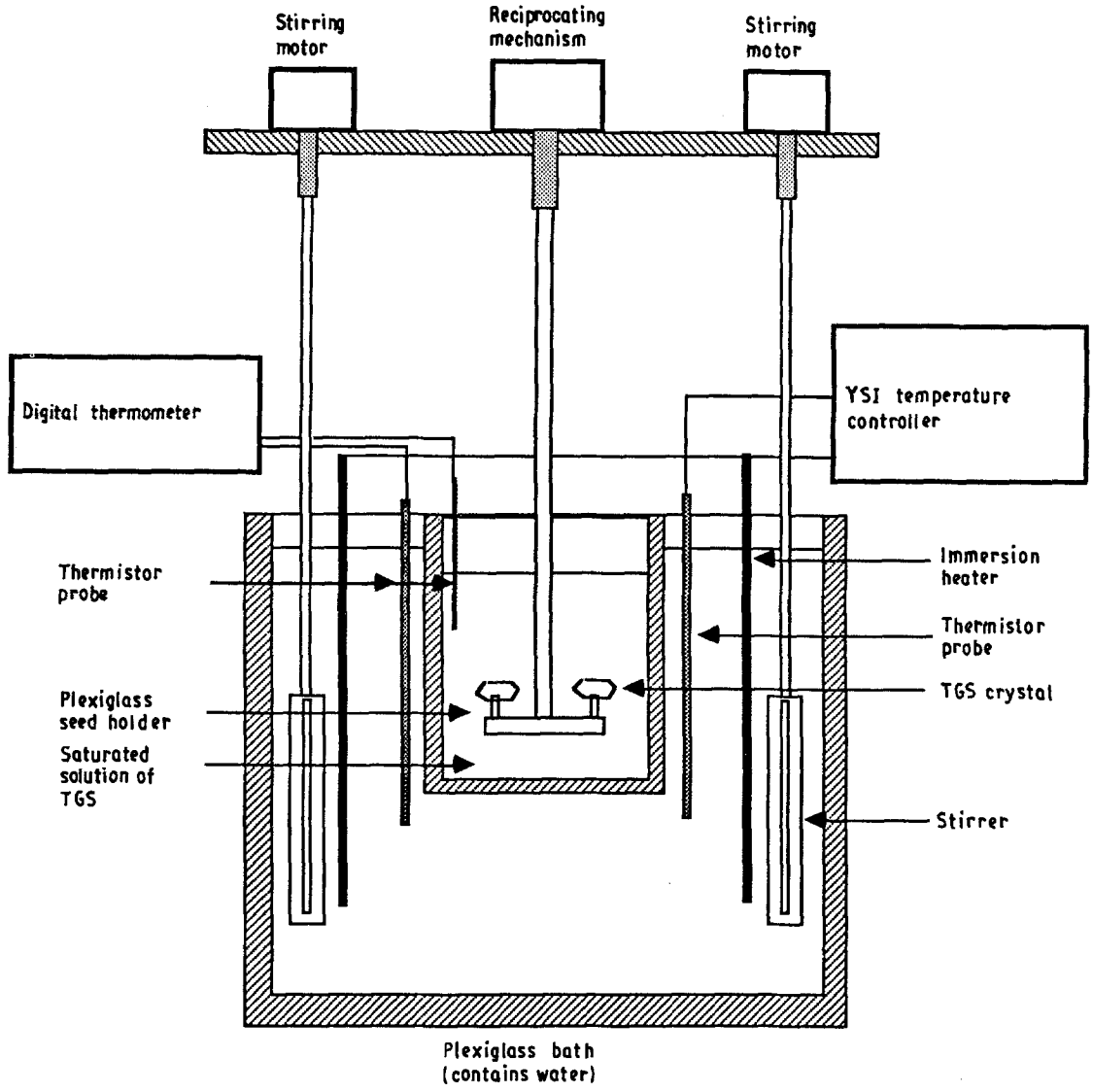

Figure 1 Schematic diagram of solution crystal growth apparatus.

conditions on the properties of the resulting crystals. After completion of the growth run, the crystals were removed from solution and slowly cooled to room temperature. Transparent and high optical quality crystals were generally obtained. The growth and morphology of these crystals have been reported earlier [17].

In this study, thin slice of samples were cleaved perpendicular to the *b*-axis (ferroelectric axis) of pure and modified crystals. The crystal specimens were lapped and polished using fine grit, 5–3 μm, alumina polishing paper and isopropyl alcohol (IPA) as a lubricant. The polished surfaces of the rectangular samples were examined under optical microscope for any induced defects, and finally polished by water and trichloroethylene solution to remove any polishing residue. Silver electrodes were thermally evaporated on to the major faces (0 1 0) of the crystal. After applying the electrodes and before the electrical measurements, the samples were kept at 60 °C for 48 h to remove any moisture present.

The block diagram of complete electrical characterization set up and three-terminal sample holder [18] used is shown in Fig. 2. The electroded sample was held between two low-tension spring-loaded gold-coated electrodes, to avoid any piezoelectric pick up. A 3 in. ($\sim$ 76.2 mm) diameter copper block, with 1000 mm^3 cavity, wrapped with a 500 W band heater was used to obtain a uniform temperature of the samples. The temperature of the sample holder was controlled using a YS1-72 proportional temperature controller and could be varied at any desired rate (0.05–1 °C min^{-1}) by applying suitable voltage to the band heater. The sample temperature was monitored using a YS1-700 series thermister to an accuracy of $\pm$ 0.05 °C. Prior to the electrical measurements, the samples were poled to eliminate multi domains, an inert problem in TGS, which might be superimposed on the effects of the dopant on the crystal's electrical properties. For poling, an electric field of 4 kV cm^{-1} was applied across the electroded sample during slow cooling from above the Curie temperature (52 °C) down to room temperature. A 1618 General Radio Automatic Capacitance Bridge was used to measure directly the sample capacitance and dissipation factor of crystal samples, during a heating cycle of 24–54 °C at a heating rate of 0.08–0.1 °C min^{-1}, with an a.c. field of 6 V cm^{-1} at 1 kHz frequency.

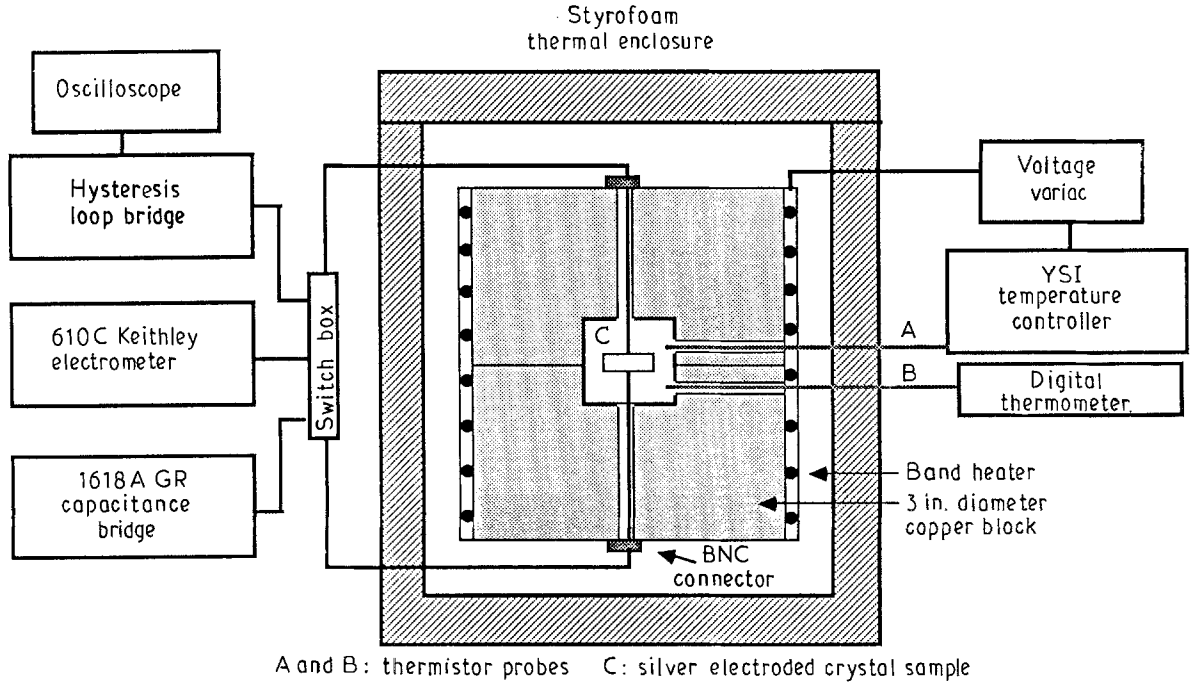

Figure 2 Schematic diagram of electric characterization set up.

A modified version of a Sawyer–Tower Bridge [18, 19] was fabricated and used to determine the spontaneous polarization and coercive field of crystal samples by direct measurement of vertical and horizontal intercepts of a saturated loop. The hysteresis loops for pure and doped crystals, were obtained by a 60 Hz a.c. field varying from 100–3000 V cm^{-1} depending on the domain state of the samples. The pyroelectric current in these samples was measured by direct method of Byer and Roundy [20]. The details of calculation of various electrical parameters are described elsewhere [18].

3. Figures of merit for pyroelectric detector targets

The performance of a pyroelectric target is strongly dependent on its material properties. The responsivity and detectivity figures of merit [21] proposed for assessing characteristics of a single-element pyroelectric detector, operating in an optimum manner are

$$R_v = Fp/wC_pA\varepsilon' \quad (1)$$

$$R_i = Fp/C_pa \quad (2)$$

and

$$D^* = Fp(4KT)^{-1/2}/\sigma^{1/2}C_p^{1/2}. \quad (3)$$

where F is the fraction of incident power which thermalizes in the crystal, p the pyroelectric coefficient, C_p the specific heat at constant pressure, a the area, A the thickness of the element, ε' the real part of the dielectric constant, and σ the measured conductivity. In practice, the a.c. conductivity is usually dominated by the dielectric loss (ε'', the imaginary part of the dielectric constant) and one can write $\sigma = \omega\varepsilon''$. From these figures of merit, it is clear that optimizing its performance involves optimizing both the detector geometry and materials characteristics. In optimizing the materials characteristics, the dielectric constant and loss, and the pyroelectric coefficient must be considered together. So one can write materials figures of merit as

$$M_1 = p/C_p\varepsilon' \quad (4)$$

for high-voltage responsivity

$$M = p/C_p \quad (5)$$

for high-current responsivity

$$M_2 = p/C_p(\varepsilon'')^{1/2} \quad (6)$$

and one more figure of merit for vidicons application in [22]

$$M_3 = p/(\varepsilon')^{1/2} \quad (7)$$

These figures of merit are calculated in the present paper, assuming that specific heat capacities of different crystals do not vary greatly. The usefulness of materials for specific applications does not necessarily depend on these figures of merit alone. The other consideration such as mechanical strength, chemical stability, power of handling abilities and growth and ease of fabrication are also important.

4. Results

Figs 3–9 depict the dielectric constant, ε', dielectric loss, ε'', pyroelectric coefficient, p, hysteresis loops and figures of merit, respectively, of TGS crystals as a function of temperature. Hysteresis loop measurement data are collected in Table I. Tables II and III show values obtained for dielectric constant and pyroelectric coefficient of these crystals. The calculated values of various figures of merit, using the above parameters are presented in Tables IV–VI.

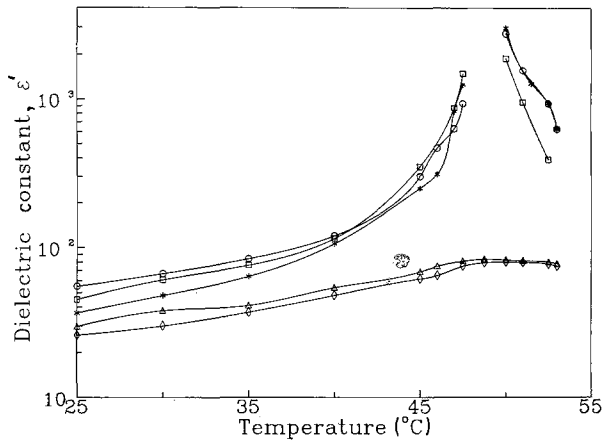

Figure 3 Dielectric constant, (ε') of pure and modified TGS crystals as a function of temperature. (*) TGS; (□) TGS + Ce; (○) TGS + Cs; (◇) TGS + L-alanine; (△) TGS + L-alanine + Cs.

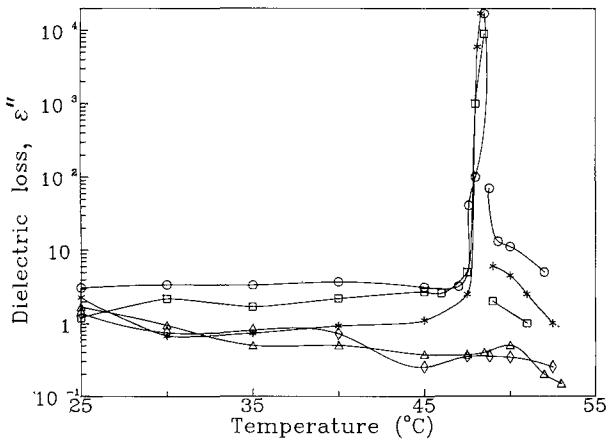

Figure 4 Dielectric loss, (ε'') of pure and modified TGS crystals as a function of temperature: (*) TGS; (○) TGS + Cs; (□) TGS + Ce; (◇) TGS + L-alanine; (△) TGS + L-alanine + Cs.

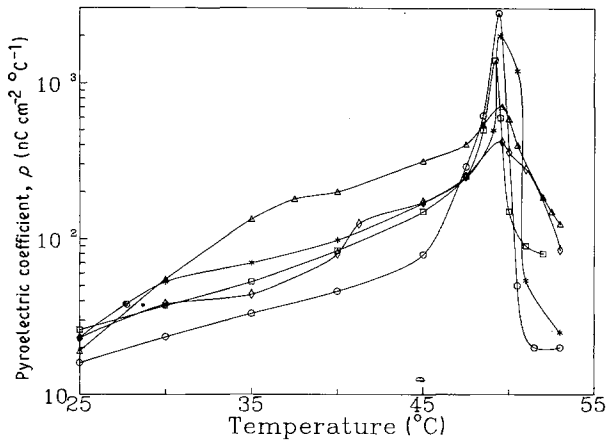

Figure 5 Pyroelectric coefficient of pure and modified TGS crystals as a function of temperature (*) TGS; (□) TGS + Ce; (○) TGS + Cs; (◇) TGS + L-alanine; (△) TGS + L-alanine + Cs.

5. Discussion

The values of ferroelectric and pyroelectric parameters and type of behaviour obtained for pure TGS crystals are in good agreement with the literature [1, 8–10, 23]. The properties of TGS vary widely in the literature because its physical properties depend on various factors, such as growth conditions, history of the sample, surface processing and electrode-forming technique, method of measurement and finally the growth pyramid from where the samples have been cut. Caesium- and cerium-doped TGS crystals exhibit higher dielectric constant and loss as compared with a pure TGS sample. Such an increase may be attributed to frittering of domains due to incorporation of these impurities into the TGS lattice. Similar results have also been observed in TGS crystals doped with copper and chromium ions [24–26]. Further, it is well known that single-domain crystals exhibit lower dielectric constant, higher spontaneous polarization, coercive field, and pyroelectric coefficient [23] than multidomain crystals. Pure, caesium- and cerium-doped TGS crystals exhibit second-order phase transition and the transition temperature of about 48.5 °C with maximum values of dielectric constant of about 75 000 and 30 000, respectively. L-alanine- and caesium + L-alanine-doped TGS crystals exhibited lower dielectric constant and loss values compared to the other three crystals studied. The dielectric constant and loss were, interestingly, suppressed in the vicinity of the transition temperature. Such behaviour indicates that the crystal remains ferroelectric beyond the expected transition point due to the presence of an internal biasing field created by substitutional incorporation of an alanine molecule into the TGS lattice. It prevents the spontaneous polarization and hence pyroelectric coefficient and dielectric constant from decreasing in the paraelectric phase, as occurs in pure TGS crystal. This is due to the internal bias present in the crystals. A similar type of behaviour is also observed by application of an external field in a proper direction. The presence of internal bias is clearly demonstrated by a ferroelectric hysteresis loop (Fig. 6) in only L-alanine and caesium + L-alanine-doped crystals. The pyroelectric coefficient and spontaneous polarization is higher than other crystals in the 30–46 °C range, which is a desirable operating temperature range for pyroelectric infrared detectors. This type of behaviour suggests that caesium + L-alanine dopants should be producing a single domain or nearly poled crystal. Moreover, the hysteresis loop observed for caesium + L-alanine-doped crystal is more symmetrical than that of the L-alanine-doped TGS crystal. It may be due to oriented incorporation of dipoles of chelate complexes of caesium with glycine or L-alanine under the influence of the electric field of the crystallization front. It can be concluded that caesium + L-alanine-doped crystals are homogeneously doped as compared with L-alanine-doped crystals. The simultaneous doping with caesium and L-alanine may also cause a sharp increase in the impurity content in the crystal, thereby creating a larger unipolar region and improved properties (Tables I–VI).

Using the data of this investigation, various figures of merit are calculated in order to judge the relative promise of using modified TGS crystal over pure crystals in infrared detector and vidicon applications. It can be seen from Tables IV–VI, that caesium + L-alanine and L-alanine-doped TGS crystals show higher values of figures of merit compared with pure, caesium- and cerium-doped TGS crystals. It is solely due to reduced dielectric constant and loss, and partially due to a slight increase in pyroelectric coefficient.

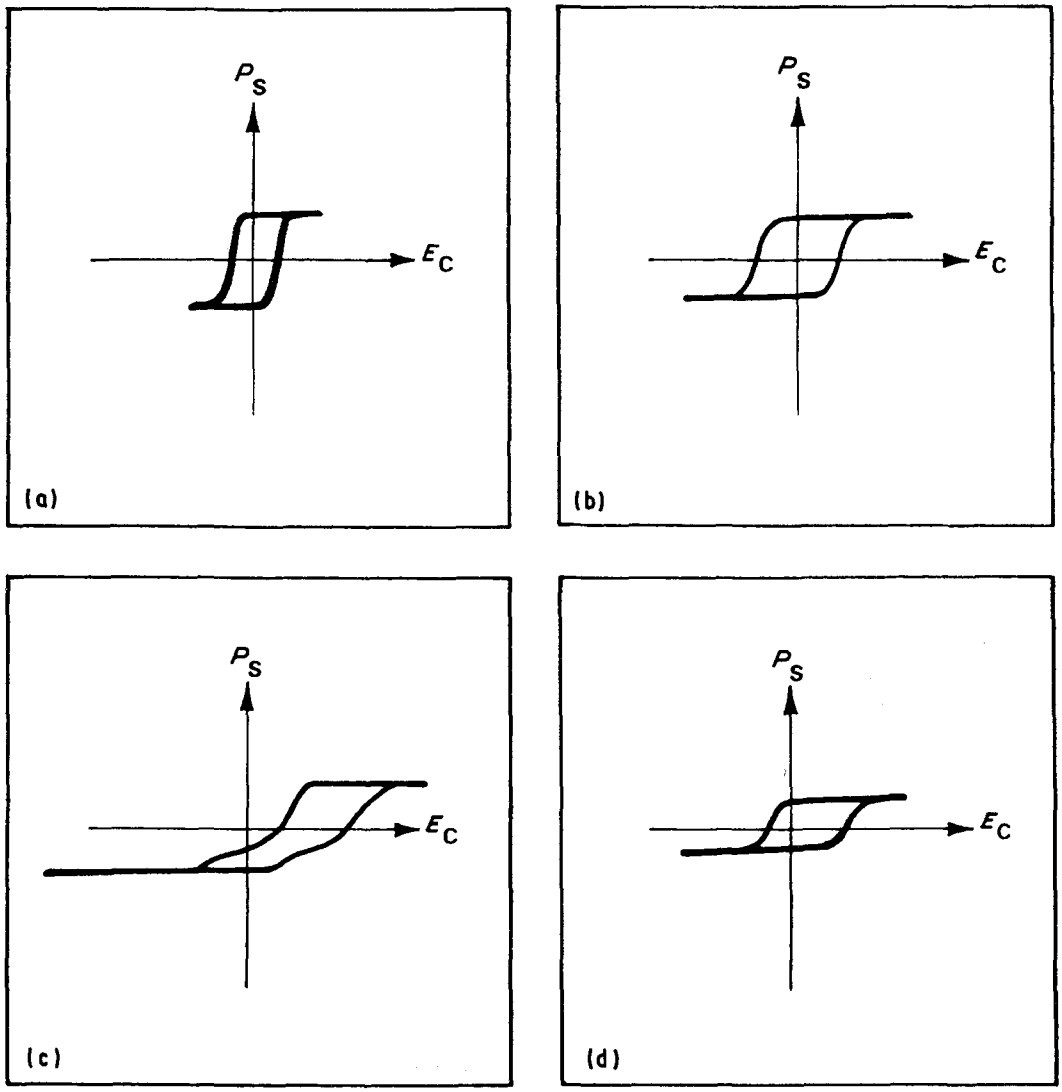

Figure 6 Ferroelectric hysteresis loop of TGS crystals (a) virgin TGS, (b) TGS + L-alanine, (c) TGS + Cs, (d) TGS + Cs + L-alanine.

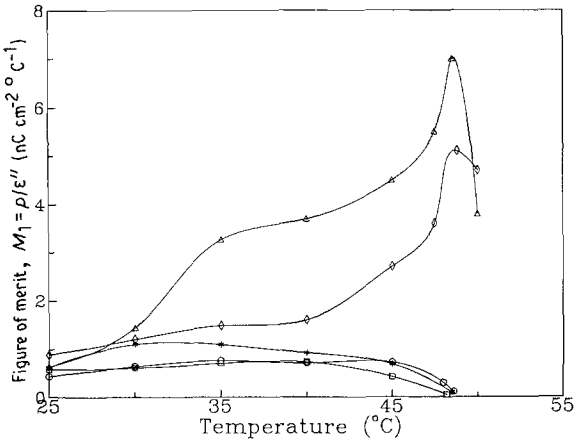

Figure 7 Figure of merit ($M_1 = p/\varepsilon''$) for I.R. detector responsivity of pure and modified TGS crystals as a function of temperature. (*) TGS; (○) TGS + Cs; (□) TGS + Ce; (◇) TGS + L-alanine; (△) TGS + L-alanine + Cs.

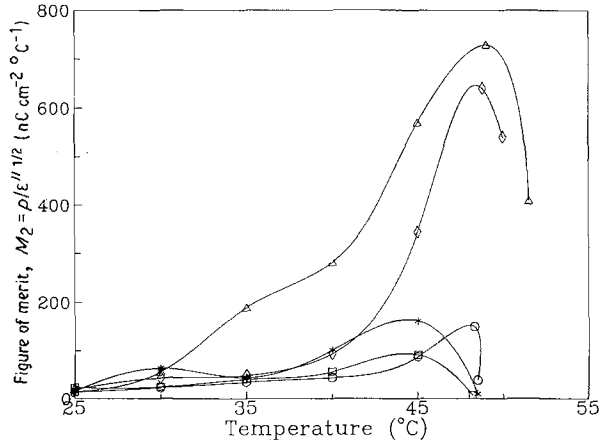

Figure 8 Figure of merit ($M_2 = p/\varepsilon''^{1/2}$) for I.R. detector detectivity of pure and modified TGS crystals as a function of temperature. (*) TGS; (○) TGS + Cs; (□) TGS + Ce; (◇) TGS + L-alanine; (△) TGS + L-alanine + Cs.

It can be concluded that L-alanine-doped TGS, especially in the presence of caesium, may be a more promising material for infrared detector applications, with a higher temperature range of operation and without degrading the performance parameters, compared to other crystals studied. L-alanine-doped crystals possess good mechanical strength but crack during cleaving and polishing. The crystal doped with L-alanine and caesium possesses better mechanical strength and hence did not crack during polishing. Further improvement in pyroelectric performance in the above-mentioned crystal may be possible by incorporating a higher concentration of these dopants into the TGS lattice. The research work in this direction is in progress. However, actual use of the above crystals in infrared detectors or vidicon tubes will

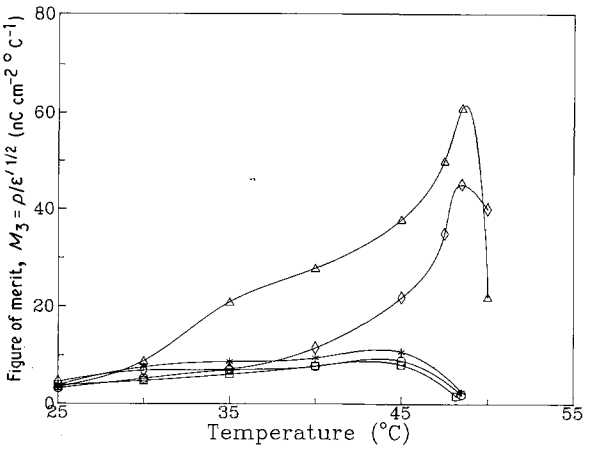

Figure 9 Figure of merit ($M_3 = p/\varepsilon'^{1/2}$) for I.R. vidicon responsivity of pure and modified TGS crystals as a function of temperature. (*) TGS; (○) TGS + Cs; (□) TGS + Ce; (◇) TGS + L-alanine; (△) TGS + L-alanine + Cs.

TABLE I Summary of hysteresis loop data of pure and modified TGS crystals

Crystals	Temp (°C)	Saturation field (V cm^{-1})	Spontaneous polarization (10^{-6} C cm^{-2})	Coercive field (V cm^{-1})
Pure TGS	25.61	1500	2.8	464
TGS + Ce	25.65	1039	2.7	466
TGS + Cs	25.7	1010	2.5	396
TGS + L-alanine	25.67	2750	2.84	704
TGS + L-alanine + Cs	25.15	2800	3.1	1290

TABLE II Dielectric constant (ε') of pure and modified TGS crystals

Crystals	Dielectric constant at				
	25 °C	30 °C	35 °C	40 °C	45 °C
Pure TGS	36.6	48	64	106	250
Caesium-doped TGS	55	67	84	120	300
Cerium-doped TGS	45	61	76	115	350
L-alanine-doped TGS	26	30	37	48	62
L-alanine + caesium-doped TGS	29.7	38	41	54	69

TABLE III Pyroelectric coefficient (p) of pure and modified TGS crystals

Crystals	Pyroelectric coefficient at				
	25 °C	30 °C	35 °C	40 °C	45 °C
Pure TGS	23	53	70	98	170
Caesium-doped TGS	24	43	64	85	155
Cerium-doped TGS	26	37	53	84	150
L-alanine-doped TGS	23	38	44	80	172
L-alanine + caesium-doped TGS	19	55	134	200	315

TABLE IV Figure of merit ($M_1 = p/\varepsilon'$) of pure and modified TGS crystals

Crystals	M_1 at				
	25 °C	30 °C	35 °C	40 °C	45 °C
Pure TGS	0.62	1.1	1.09	0.92	0.68
Caesium-doped TGS	0.436	0.64	0.76	0.708	0.52
Cerium-doped TGS	0.58	0.61	0.7	0.73	0.42
L-alanine-doped TGS	0.88	1.2	1.48	1.6	2.7
L-alanine + caesium-doped TGS	0.63	1.44	3.26	3.7	4.5

TABLE V Figure of merit ($M_2 = p/\varepsilon''^{1/2}$) of pure and modified TGS crystals

Crystals	M_2 at				
	25 °C	30 °C	35 °C	40 °C	45 °C
Pure TGS	15.1	64	44.2	101.6	162
Caesium-doped TGS	13.6	23.3	34.86	44.18	88.0
Cerium-doped TGS	23.7	25.08	40.65	56.63	91.8
L-alanine-doped TGS	19.4	43.8	48.76	94.2	345
L-alanine + caesium-doped TGS	14.5	56.4	189.5	282	570

TABLE VI Figure of merit ($M_3 = p/\varepsilon'^{1/2}$) of pure and modified TGS crystals

Crystals	M_3 at				
	25 °C	30 °C	35 °C	40 °C	45 °C
Pure TGS	3.8	7.6	8.75	9.5	10.75
Caesium-doped TGS	3.2	5.2	6.98	7.75	8.94
Cerium-doped TGS	3.86	4.76	6.08	7.83	8.07
L-alanine-doped TGS	4.5	6.9	7.23	11.54	21.84
L-alanine + caesium-doped TGS	3.48	8.9	20.9	27.9	37.9

determine if the predicted improvement in signal to noise ratio is realized.

Acknowledgements

The authors thank National Aeronautics and Space Administration for the support of this work through contracts NAS8-32945 and NASA-CCDS grant no. 375-559-3 from the Center of Crystal Growth in Space, Clarkson University, Potsdam, New York; Drs William Wilcox, Amar Bhalla, Manmohan Aggarwal, and R. F. Paulson for useful comments and discussion; Lloyd Sharp and Milford K. Lands for fabricating the crystallizer and electronic circuit for the reciprocating motion of the seed holder, respectively; and Vetrea Ruffin for typing the manuscript.

References

1. B. T. MILLER and J. P. REMEIKA, *Phys. Rev.* **104** (1956) 849.
2. E. A. WOOD and A. N. HOLDEN, *Acta Crystallogr.* **10** (1957) 145.

3. S. HOSHINO, Y. OKAYA and R. PEPINSKY, *Phys. Rev.* **2** (1959) 15.
4. H. P. BEERMAN, *IEEE Trans. Elect. Dev.* **16** (1968) 554.
5. E. H. PUTLEY, "Semiconductors and Semimetals", Vol. 5 (Academic Press, New York, 1970).
6. P. W. KRUSE, L. D. McGLANCHLIN and R. B. McQUINSTAN, "Elements of Infrared Technology" (Wiley, New York, 1962).
7. P. J. LOCK, *Appl. Phys. Lett.* **19** (1971) 390.
8. A. K. BATRA and S. C. MATHUR, *Ferroelectrics* **49** (1983) 219.
9. C. S. FANG, A. S. BHALLA, L. E. CROSS and Y. XI, *Mater. Sci. Lett.* **2** (1983) 134.
10. A. S. BHALLA, C. S. FANG, Y. XI and L. E. CROSS, *Appl. Phys. Lett.* **43** (1983) 932.
11. K. ZHANG, J. SONG, M. WAND, C. FANG and M. LU, *J. Crystal Growth* **82** (1987) 639.
12. M. A. GAFFAR and A. E. A. AZIZ, *Arab Gulf J. Sci. Res. Math. Phys. Sci.* **A5(2)** (1987) 271.
13. R. B. LAL and A. K. BATRA, Annual Report, NASA-CCDS No. 375-559-3 to Center of Crystal Growth and Space at Clarkson University, NY (1987–88).
14. P. F. PAULSON, Barnes Engineering Division, EDO Corporation, CT, USA, private communication (1989).
15. R. B. LAL, M. D. AGGARWAL, A. K. BATRA and R. KROES, Final Report, NAS8-32945 submitted to National Aeronautics and Space Administration, USA (1987).
16. M. D. AGGARWAL and R. B. LAL, *Rev. Sci. Instrum.* **54** (1983) 722.
17. M. BANAN, A. K. BATRA and R. B. LAL, *J. Mater. Sci. Lett.* **8** (1989) 1348.
18. M. BANAN, A. K. BATRA, R. B. LAL and M. D. AGGARWAL, in "Proceedings/Abstracts of ACHE-9th Annual Science Symposium", Alabama State University, Montgomery, Alabama, USA, April, 1985, M. Banan, M. S. Thesis, Alabama A & M University, Normal, AL (1986).
19. C. B. SAWYER and C. H. TOWER, *Phys. Rev.* **35** (1930) 269.
20. R. L. BYER and C. B. ROUNDY, *Ferroelectrics* **3** (1972) 333.
21. M. E. LINES and A. M. GLASS, "Principle and Applications of Ferroelectrics and Related Materials" (Clarenden Press, Oxford, 1977).
22. R. G. F. TAYLOR and H. A. H. BOOT, *Contemp. Phys.* **14** (1973) 55.
23. A. K. BATRA, PhD Thesis, Indian Institute of Technology, Delhi, India (1982).
24. N. D. GAVILLOVA and T. V. DERHENEVA, *Sov. Phys. Crystallogr.* **26** (1981) 236.
25. F. MORVAC and J. NOVOTRY, *Kristall and Technik* **6** (1971) 335.
26. M. S. TRESDRIK and E. M. DRARCHENVA, *ibid.* **11** (1976) 49.

Received 12 December 1989
and accepted 6 June 1990